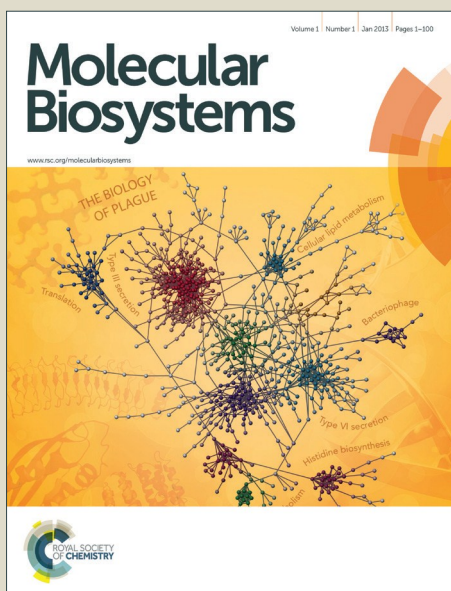


Molecular BioSystems

Accepted Manuscript



This is an *Accepted Manuscript*, which has been through the Royal Society of Chemistry peer review process and has been accepted for publication.

Accepted Manuscripts are published online shortly after acceptance, before technical editing, formatting and proof reading. Using this free service, authors can make their results available to the community, in citable form, before we publish the edited article. We will replace this *Accepted Manuscript* with the edited and formatted *Advance Article* as soon as it is available.

You can find more information about *Accepted Manuscripts* in the [Information for Authors](#).

Please note that technical editing may introduce minor changes to the text and/or graphics, which may alter content. The journal's standard [Terms & Conditions](#) and the [Ethical guidelines](#) still apply. In no event shall the Royal Society of Chemistry be held responsible for any errors or omissions in this *Accepted Manuscript* or any consequences arising from the use of any information it contains.



www.rsc.org/molecularbiosystems



Journal Name

ARTICLE

Identification and localization of Xylose-binding proteins and as potential biomarkers for liver fibrosis/cirrhosis

Yaogang Zhong,^a Xiu-Xuan Sun,^b Peixin Zhang,^a Xinmin Qin,^a Wentian Chen,^a Yonghong Guo,^c Zhansheng Jia,^d Huijie Bian,^{*b} Zheng Li^{*a}

Received 00th January 20xx,
Accepted 00th January 20xx

DOI: 10.1039/x0xx00000x

www.rsc.org/

In our recent study, we found the expression levels of total Xylose-binding proteins (XBPs) were up-regulated significantly in the activated hepatic stellate cells (HSCs), however, the denomination, distribution, and function of XBPs were uncharted. Here, 70 XBPs from the activated HSCs and 64 XBPs from the quiescent HSCs were isolated, identified and annotated. A total of 30 XBPs were up-regulated (all fold change ≥ 1.5 , $p \leq 0.05$) and 14 XBPs were down-regulated (all fold change ≤ 0.67 , $p \leq 0.05$) in the activated HSCs. The XBPs were localized at the cytoplasm and cytoplasmic membrane in HSCs and cirrhotic liver tissues by cy/histochemistry. The XBPs (i.e., PDIA6 and CFL2) responsible for the regulation of protein binding were up-regulated, and those (i.e., TUBB and MX1) responsible for the regulation of catalytic activity were up-regulated in the activated HSCs. Then, 2 candidates (e.g., PDIA6 and APOA1) were selected for further verification in the sera of HBV-induced chronic hepatitis/cirrhosis using western blotting and serum microarrays. Assessments of PDIA6 and APOA1 as biomarker candidates show a higher discrimination (Area Under Curves, AUCs = 0.8985, $p < 0.0001$) relative to APOA1 (AUCs = 0.8738, $p < 0.0001$) in sera of patients. In conclusion, the precision alteration of the XBPs referred to pathological changes in HSCs during liver fibrosis/cirrhosis may provide pivotal information to discover the potential glycan-binding proteins related biomarkers for diagnosis of liver fibrosis/cirrhosis and development of new anti-fibrotic strategies.

1. Introduction

Carbohydrates decorate the surfaces of all living cells and comprise highly diverse structures that play an important role in many biological process including cell-cell interactions, signaling and immune responses. These distinct structural elements govern interactions with other molecules such as glycan-binding proteins (GBPs), which also play important roles in mechanisms of immunity and microbe-host interactions through glycan recognition.¹⁻³ An expanding number of mammalian GBPs have been identified and are classified by sequence motifs such as C-type lectins,⁴ S-type lectins,⁵ P-type lectins,⁶ and the Siglecs.⁷ However, the xylose-specific lectin remain poorly reported.

D-Xylose (Xyl) is a five-carbon aldose (pentose, monosaccharide) that can be catabolized or metabolized into

useful products by a variety of organisms. An oxido-reductase pathway is present in eukaryotic microorganisms.⁸ The Weicker, *et al.* reported that the Xyl was found in the glycoproteins isolated from the urine of patients with inflammatory processes, tumors, plasmacytomas.⁹ Yang, *et al.* detected and testified the occurrence of the Xyl in the human sera, especially over-expressed in the hepatocellular carcinoma cases.¹⁰ The Xyl-binding proteins (XBPs) is a class of periplasmic proteins that binding Xyl with high affinity, and is a component of the Xyl transporter gene (XylFGH) carrier system that translocates Xyl into the cytoplasm.¹¹ The XylFGH operon represents the ATP binding cassette transport system with the periplasmic XBPs, and membrane permease encoded as XylF, XylG, and XylH, respectively.^{12,13} However, the interactions between the XBPs and specific Xyl types remain poorly understood.

Liver fibrosis is the excessive accumulation of extracellular matrix (ECM) proteins including collagen that is a characteristic of most types of chronic liver diseases.¹⁴ The main causes of liver fibrosis in industrialized countries include chronic hepatitis B/C virus infection, nonalcoholic steatohepatitis, and alcohol abuse.¹⁵ The main liver cells that produce matrix are hepatic stellate cells (HSCs). HSCs exist in a resting phenotype as the body's major store of vitamin A. However on activation they transform to adopt a myofibroblast phenotype capable of secreting collagen.¹⁶ This activation process is driven by two cytokines (transforming growth factor- β 1 (TGF- β 1) and platelet-derived growth factor), leading to the increased expression of contractile filaments.¹⁷ TGF- β 1 is a polypeptide member of the transforming growth factor beta superfamily of cytokines. It is a secreted protein that performs

^aLaboratory for Functional Glycomics, College of Life Sciences, Northwest University, Xi'an 710069, P. R. China

^bCell Engineering Research Centre and Department of Cell Biology, Fourth Military Medical University, Xi'an 710032, P. R. China

^cDepartment of infectious diseases, The second Hospital of Medicine college of Xi'an Jiaotong University, Xi'an 710004, P. R. China

^dCenter of infectious diseases, Tangdu Hospital, Fourth Military Medical University, Xi'an, P. R. China

*Corresponding author: Prof. Zheng Li, Ph.D., Laboratory for Functional Glycomics, College of Life Sciences, Northwest University, No. 229 Taibai Beilu, Xi'an 710069, China. Fax: +86-29-88303572; E-mail: zhengli@nwwu.edu.cn and Prof. Huijie Bian, Ph.D., Cell Engineering Research Centre and Department of Cell Biology, Fourth Military Medical University, No.169 Changle Xilu, Xi'an 710032, China. Fax: +86-29-84774480; E-mail: hjbian@fmmu.edu.cn

†Electronic Supplementary Information (ESI) available: See DOI: 10.1039/x0xx00000x

many cellular functions, including adipogenesis, myogenesis, chondrogenesis, osteogenesis, cell growth, cell proliferation, epithelial cell differentiation and apoptosis, and immune. LX-2 is a low-passaged HSCs cell line derived from normal HSCs that are spontaneously immortalized, which can be activated by TGF- β 1.¹⁴⁻¹⁷ Our previous research results have shown 12 carbohydrates (e.g., Xyl, Gal, GalNAc and Man-9Glycan) showed increased signal, while 7 carbohydrates (e.g., NeuAc, Lac and GlcNAc-O-Ser) showed decreased signal in the activated LX-2, meanwhile, the expression levels of total XBPs were up-regulated significantly (fold change = 3.23, $p \leq 0.0001$) in the activated LX-2 using a carbohydrate microarray.¹⁸

In this study, an experimental strategy (Scheme 1 (ESI[†])) was designed relying on the use of a carbohydrate microarray and LC-Orbitrap MS/MS. First the expression levels of total XBPs from the quiescent and activated LX-2 were detected by carbohydrate microarrays, and validated using the carbohydrate cytochemistry. Second the XBPs were isolated by Xyl-magnetic particle conjugates (XMPCs), and identified by LC-Orbitrap MS/MS. The localization of the identified XBPs were validated in HSCs and cirrhotic liver tissues by cy/histochemistry. Then, an in-depth functional analysis for the identified XBPs in HSCs was performed. Finally, the relevance of the XBPs as potential biomarkers were investigated in sera of HBV-induced chronic hepatitis/cirrhosis samples by western blotting and serum assays.

2. Materials and methods

2.1. Cell line and culture

LX-2 was provided by Dr. Friedman of Mount Sinai School of Medicine, New York, USA. The cells were grown in DMEM containing 10% FBS, 100 U/mL penicillin and 100 mg/mL streptomycin (all reagents were purchased from Invitrogen, Carlsbad, CA, USA).

As for preparation of fibrosis models, LX-2 was grown in DMEM containing 2% FBS, 100 U/mL penicillin, 100 mg/mL streptomycin and 2 ng/mL TGF- β 1.¹⁹ The cell lines were maintained at 37°C in 5% CO₂. After 24 h of TGF- β 1 stimulation, the activated and quiescent HSCs were lysed for total protein extraction or fixed for further cytochemistry.

2.2. Serum and tissues samples collection

The collection of human blood and tissues were performed in accordance with approved guidelines. The collection and use of all human pathology specimens for research presented here were approved by the Ethical Committee of Northwest University, Fourth Military Medical University and Xi'an Jiaotong University (Xi'an, China). Written informed consent was received from participants for the collection of their blood and tissues. This study was conducted in accordance with the ethical guidelines of the Declaration of Helsinki. Epidemiologic and clinical data from patients and normal was collected by questionnaire and from medical reports. The characteristics of all study participants were summarized in Table S1 (ESI[†]).

Serum samples were immediately separated from the clotted whole blood by centrifugation at 1,500 \times g for 10 min at 4°C. After centrifugation, the samples were divided into 100 μ L aliquots in cryotubes, and stored at -80°C until use. Cirrhotic liver tissues were obtained during the surgical resection and were snap-frozen in liquid nitrogen and stored at -80°C until used. All of the liver samples were histologically examined by

hematoxylin and eosin staining and confirmed by experienced pathologists.

2.3. Isolation and identification of XBPs

Isolation and identification of XBPs was performed according to the method published before.²⁰ The detailed information was provided in the Electronic Supplementary Information.

2.4. Validation of localization by immunocytochemistry

Immunocytochemical staining was performed according to the method published before.¹⁸ Immunocytochemistry was performed by primary antibody (diluted 1:500) obtained from Epitomics (Burlingame, CA, USA), Cy3/Cy5 fluorescent-conjugated secondary antibodies (diluted 1:1000) (Haimen, China) was used according to the protocol.^{18,20} Finally, the cells were stained with 1 μ g/mL DAPI (Roche; Basel, Swatzerland) and scanned by Laser Scanning Confocal Microscope (LSCM) (NIKON, Tokyo, Japan). The staining results were repeated at least three times. The representative pictures were showed in related figures.

2.5. Validation of the expression of XBPs by Western blotting analysis

Western blotting was performed as described previously.²¹ Briefly, 50 μ g of protein from HSCs and sera samples was separated by 10% SDS-PAGE and transferred to a PVDF membrane (Millipore). After incubating overnight at 4°C with rabbit monoclonal antibodies (Burlingame, CA, USA, diluted 1:500-1:1000). The membranes were washed three times with TBST (100 mmol/L Tris-HCl, 150 mmol/L NaCl, 0.05% Tween-20, pH 7.4) and incubated with alkaline phosphatase-conjugated secondary antibodies (diluted 1:1000) for 2 h at room temperature. Relative protein expression was detected using the BCIP/NBT substrate kit (Beyotime Institute of Biotechnology) in each sample.

2.6. Serum microarrays

A Serum microarray was produced according to our previous protocols^{22,23} with some modifications. In total, 54 individual serum samples from normal (n = 27) and patients with HBV-induced chronic hepatitis/cirrhosis (n = 27) were dissolved in PBS (10 mmol/L phosphate buffer containing 150 mmol/L NaCl, pH 7.4) to a concentration of 1 mg/mL before spotting on homemade epoxysilane-coated slides with Stealth micro spotting pins (SMP-10B). After immobilization, the slides were blocked with 5% BSA. Primary antibody (diluted 1:500) was incubated on the blocked slide for 3 h at room temperature. After that, Cy3 fluorescent-conjugated secondary antibodies (diluted 1:1000) (Haimen, China) was used. Then, the slide was scanned using a Genepix 4000B confocal scanner, and the acquired images were analyzed at 532 nm for Cy3 detection, which was performed as previously described.²³

3. Results

3.1. Expression level and localization of XBPs in HSCs

Currently, α -smooth muscle actin (α -SMA)-positive HSCs can be distinguished from other portal, interface and septal myofibroblasts by their specific position in the liver perisinusoidal space.¹⁴ In this study, HSCs were activated by 2 ng/mL TGF- β 1 (Fig. 1A), the correlation between the degree of α -SMA immunoreactivity of the perisinusoidal region and the

Child–Pugh score was significant ($p < 0.001$), which is consistent with another report that α -SMA expression of HSCs reflects liver fibrosis progression.¹⁴

Our previous research results have demonstrated that the expression levels of total XBPs were up-regulated significantly in the activated HSCs,¹⁸ however, their denomination and distribution in HSCs were uncharted. Here, Cy3-labeled Xyl was used to further validate the results as well as assess the XBPs distribution in HSCs using the carbohydrate cytochemistry. Besides, carbohydrate competitive inhibition (The mixture of equal parts of Cy3- and non-labeled Xyl) assays were used as the negative control. The Xyl exhibited moderate scattered particle-like signals in the cytoplasmic membrane and strong binding to the central cytoplasm and/or the perinuclear cytoplasm in the quiescent LX-2 (Fig. 1Ba1-a2), and the binding intensified in the same regions of the activated LX-2 (Fig. 1Bb1-b2). The competitive inhibition of Xyl showed moderate binding to the same region with Xyl staining (Fig. 1Ba3-a4, Q: $p < 0.01$ and 1Bb3-b4, A: $p < 0.001$).

Fig. 1 Confocal microscopy. (A) LX-2 was incubated with 2 ng/mL of TGF- β 1 for 24 h and determination of α -SMA expression in Q (Untreated) and A (TGF- β 1). (B) The localization of XBPs and the competitive inhibition assay of Xyl in Q (Untreated) and A (TGF- β 1). * $p < 0.05$, ** $p < 0.01$, *** $p < 0.001$.

3.2. Identification and GO analysis of XBPs

The isolated XBPs (6 μ g) were resolved by SDS-PAGE and visualized by silver staining, which exhibited the apparent bands between 100 kDa and 20 kDa (Fig. 2A). After that, The XBPs were digested by trypsin, then identified by LC-Orbitrap MS/MS. The results were analyzed and compared using the Proteome Discoverer 1.2 software (Thermo Fisher) with SEQUEST search. All MS/MS spectra were searched from the International Protein Index (IPL.HUMAN. v3.73. Fasta) with the following parameters: A mass tolerance of ± 10 ppm for the precursor ions and a tolerance of ± 1 Da for fragment ions were used. Differential expressed proteins presented in the activated and quiescent LX-2 were listed in Table S2 (ESI \dagger). A total of 158 and 143 unique peptides covered 64 and 70 XBPs were identified from the quiescent and activated LX-2, respectively (Fig. 2B (left)). It was noticed that there was an overlap of 46 (52.3%) XBPs between the activated and quiescent LX-2, while 18 (20.5%) and 24 (27.3%) XBPs only identified from the quiescent and activated LX-2, respectively (Fig. 2B (right)).

To investigate the major biological functions of XBPs, Blast2GO^{24,25} and WEGO²⁶ were applied to analyze the total unique proteins for functional enrichment according to three grouping classifications: biological processes, cellular components, and molecular functions (Fig. 2C–2E). Of 88 identified XBPs, 81 had GO annotations available. In terms of biological processes, 12 proteins (14.0%) and 11 proteins (13.0%) were included in cellular process and single-organism process, respectively. In terms of cellular components, 24 proteins (27.0%) were cell proteins and 21 proteins (24.0%) were organelle proteins. In terms of molecular function, proteins with binding ability formed the largest group (46, 52%) and other smaller groups identified included catalytic activity (22, 25.0%) and structural molecule activity (16, 18.0%). The top three most common binding were protein binding (26.0%), heterocyclic compound binding (16.0%) and organic cyclic compound binding (16.0%) (Fig. 2E). The main catalytic activity categories were signal transducer activity (28.0%), enzyme inhibitor activity (9.0%) and laminin receptor activity (9.0%) (Fig. 2E). In order to further study its functions

on a macro level, the WEGO were further used to analyze the identified XBPs, the result showed that the function was no distinction between the activated and quiescent LX-2 (Fig. S2 (ESI \dagger)).

Fig. 2 Identification of the isolated XBPs. (A) SDS-PAGE analysis. Lane 1: The quiescent LX-2 proteins; Lane 2: The activated LX-2 proteins; Lane 3 and Lane 4: Protein fraction not bound to xylose; Lane 5 and Lane 6: Washing composition; Lane 7: The eluted fraction of quiescent LX-2 proteins. Lane 8: The eluted fraction of activated LX-2 proteins. (B) Cross-correlation of the isolated peptides (Left) and XBPs (Right) presented in the Venn diagram from the quiescent and activated LX-2. GO classification of the identified XBPs using Blast2GO (C) Biological process (D) Cellular component; (E) Molecular function level.

3.3. KEGG pathway and network analysis

In total, 44 of 88 identified XBPs were annotated in DAVID Bioinformatics Resources (version 6.7),²⁷ and KEGG pathway.²⁸ The XBPs were mainly mapped to 15 KEGG pathways (e.g., Glycolysis/Gluconeogenesis (Fig. 3A), Protein processing in ER (Fig. 3B), and Antigen processing and presentation (Fig. 3C)) with thresholds of count ≥ 1.5 and a P -value ≤ 0.05 versus the background signal of the human genome (Table S3 (ESI \dagger)). For example, in Glycolysis/Gluconeogenesis pathway, expression of prohibitin-2 (PHB2), 60 kDa heat shock protein (HSPD1), and 28S ribosomal protein S9 (MRPS9) (all fold change ≥ 2.99 , $p \leq 0.05$) were up-regulated significantly, while expression of protein disulfide-isomerase (P4HB), and 14-3-3 protein beta/alpha (YWHAB) (both fold change ≤ 0.67 , $p \leq 0.05$) were down-regulated, which probably resulted in increased glycerate-1,3P2, glycerate-2,3P2, glycerate-3P and phosphoenolpyruvate, and decreased L-Lactate in the activated LX-2. In addition, the 43 matched XBPs were queried against the STRING Homo sapiens database to determine their functional relevance. Through enrichment analysis of molecular function, more than 27 proteins responsible for protein binding exhibited significant alteration (17 proteins, fold change ≥ 1.5 ; 7 proteins, fold change ≤ 0.67), and 9 proteins responsible for catalytic activity showed increased expression in the activated LX-2 (all fold change ≥ 1.5 , $p \leq 0.05$) (Fig. S3A and S3B (ESI \dagger)).

Fig. 3 Functional analysis in HSCs. KEGG pathway analysis of the identified XBPs (marked with red) that were mapped to Glycolysis/Gluconeogenesis (A), Protein processing in endoplasmic reticulum (B) and antigen processing and presentation (C) pathways.

3.4. Sequence motif preference of XBPs

The characteristics of the isolated XBPs were analyzed according to their exhibiting consensus sequence with motif-x software (v1.2 10.05.06).²⁹ Herein, the data set provided a good basis to test the generality of motifs and identify further consensus sequences of XBPs. The position-specific amino acid frequencies of the surrounding each of normal amino acids (13 amino acids to both termini) were compared with the background. Notably, 9 specific nonredundant consensus sequences with a high motif score and fold increase ≥ 30 were identified (Fig. 4A). [DN]C[GAM]D[GN]SDEx[PDA][CEA]xx and [DN]DC[GM]D[GN]SDEx[PA]Cx motifs (both motif score ≥ 33.67 , fold increase ≥ 30.68) (e.g. [DN] and [GAM] represent several amino acid residues that might appear in the position) were significantly overrepresented in the XBPs data. Interestingly, xxx[WL]xC[DN]G[DE][DN][DNI]C[GAM] motif (motif score = 34.32, fold increase = 39.87) were also significantly overrepresented in the XBPs data (Fig. 4B).

3.5. Validation of the expression of XBPs in HSCs and sera from HBV-induced chronic hepatitis/cirrhosis patients

Protein abundance expressed as peak area values was calculated using the area of any given protein according to the protocol.³⁰ 30 XBPs were estimated to be significantly up-regulated (all fold change ≥ 1.5 , $p \leq 0.05$) and 14 XBPs were estimated to be significantly down-regulated (all fold change ≤ 0.67 , $p \leq 0.05$) in the activated LX-2. Western blotting was employed to further confirm the expression levels of the XBPs. Such PDIA6 was up-regulated, and APOA1 was down-regulated in the activated LX-2 and sera of patients, which was markedly consistent with the results of MS analysis (Fig. 4C). Analysis of serum arrays were performed to confirm PDIA6 and APOA1 in the crude sera of patients and normal. According to the results, the expression level of PDIA6 was increased significantly in the sera of the patients. The expression level of APOA1 exhibited significant decreased signals in the sera of the patients compared with normal (Fig. 4D).

3.6. Localization of PDIA6 and APOA1 in HSCs and cirrhotic liver tissues

To determine the localization and expression levels of PDIA6 and APOA1, the double immunofluorescence analysis was performed in HSCs and cirrhotic liver tissues. The measurement of α -SMA was used as an internal control. As shown in Fig. 4E, α -SMA ($p < 0.05$) was detected at consistently higher levels in the activated LX-2 (Fig. 4Eb2 and 4Ed2) than the quiescent LX-2 (Fig. 4Ea2 and 4Ec2). Although PDIA6 is known to be expressed in and around the cytoplasm and ER in human cells,^{31,32} here, the expression level of PDIA6 was found that it was strongly and predominantly localized at the cytoplasmic membrane, the central cytoplasm and/or the perinuclear cytoplasm, especially at the perinuclear cytoplasm region. In this region, PDIA6 was expressed higher in the activate LX-2 (Fig. 4Eb3) than the quiescent LX-2 (Fig. 4Ea3). APOA1 is also known to mainly localize to the vesicles, and in the cytoplasm of some cells.³³ Here, the expression level of APOA1 was found that it was down-regulated significantly in the activated LX-2 (Fig. 4Ed3) compared with the quiescent LX-2 (Fig. 4Ec3). In addition, α -SMA was selected as a positive control for the activation of HSCs in cirrhotic tissues (Fig. 4Fa1 and 4Fb1). The expression levels of PDIA6 and APOA1 were observed in the hepatocytes and sinusoidal cells of cirrhotic liver tissue (Fig. 4Fa2 and 4Fb2). Interestingly, PDIA6 showed moderate binding to the cytoplasmic membrane, but strong binding to the cytoplasm of hepatocytes, and to the cytoplasm and cytoplasmic membrane of sinusoidal cells in cirrhotic tissues (Fig. 4Fa4 and 4Fa5). However, APOA1 showed moderate binding to the cytoplasm and cytoplasmic membrane both in the hepatocytes and sinusoidal cells of cirrhotic tissues. Thus, these results suggested the possibility that PDIA6 and APOA1 were co-expressed in the marginal region of the central cytoplasm and/or the perinuclear cytoplasm and cytoplasmic membrane liver fibrosis tissues.

3.7. Assessment of PDIA6 and APOA1 as biomarker candidates using ROC analysis

ROC curve analysis was used to determine the potential impact of PDIA6 and APOA1 as potential biomarkers for discriminating patients and normal. The area under curves (AUCs) was determined for each value alone to determine which one yielded the greatest discriminatory power within this patient set. The serum expression levels of PDIA6 had an AUCs of 0.8985 with a 95% confidence interval (0.8132 to 0.9838, $p < 0.0001$) for distinguishing patients and normal. The

serum expression levels of APOA1 resulted in an AUCs of 0.8738 with a 95% confidence interval (0.7830 to 0.9646, $p < 0.0001$) for differentiating patients and normal (Fig. 4G).

Fig. 4 Sequence motif preference for the XBPs and validation of the expression of XBPs in HSCs, individual serum samples and liver tissues. (A) List of specific nonredundant consensus sequences with a high motif score and fold increase ≥ 30 . (B) WebLogo generated relative frequency plots of the significant sequence motif. The heights of the residues are approximately proportional to their binomial probabilities. (C) Western blotting analysis of the expression levels of PDIA6 and APOA1 in HSCs and serum samples from patients and normal. (D) Schematic of protein, primary antibody, and Cy3-labeled secondary antibody binding interactions on the serum microarray. (E) The double immunofluorescence of antibody (PDIA6 and APOA1) and α -SMA in the quiescent and activated LX-2. (F) The double immunofluorescence of antibody (PDIA6 and APOA1) and α -SMA in the liver cirrhotic tissues. S, Sinusoidal cells; H, Hepatocytes cells. (G) ROC analyses for significantly changed PDIA6 and APOA1 were detected by serum arrays. The green line: PDIA6; The blue line: APOA1.

4. Discussion

Glycans possess distinct structural elements to govern interactions with the GBPs. The GBPs that act through glycan recognition are also called lectins play important roles in mechanisms of immunity and microbe-host interactions as well as are typically highly selective for specific glycan structures and have therefore been extremely useful in studying glycan variation.¹⁻³ The Xyl was found in the glycoproteins isolated from the serum and urine of patients. However, the denomination, distribution, and functions of the XBPs as well as the interactions with the specific Xyl types remain poorly understood. Liver Fibrosis is a major complication of various chronic hepatic diseases due to the increased production and decreased degradation of the ECM.⁷ The activated HSCs are considered the primary contributor of the ECM in chronic liver disease leading to liver fibrosis.⁸ In normal liver, the quiescent HSCs reside in the space of Disse and are the major storage sites of vitamin A. Following chronic liver injury, HSCs are activated and transdifferentiate into myofibroblast-like cells to acquire contractile, proinflammatory and fibrogenic properties.^{9,10} This activation process is driven by two cytokines, leading to the increased expression of contractile filaments (α -SMA), and ECM proteins (collagen Type I (Col), I, and III).^{8,11-13}

Our previous research results have demonstrated that the expression levels of total XBPs were up-regulated significantly in the activated HSCs.¹⁸ In this study, the XBPs from the activated and quiescent LX-2 were isolated and identified by XMPCs and the LC-Orbitrap MS/MS analysis, respectively. As a result, a total of 30 identified XBPs were up-regulated and 14 XBPs were down-regulated in the activated LX-2 during liver fibrosis/cirrhosis, which were localized at the cytoplasm and cytoplasmic membrane in HSCs and liver tissues by cy/histochemistry. The characteristics of the identified XBPs were analyzed according to their exhibiting consensus sequence. Notably, 9 specific nonredundant consensus sequences with a high motif score and fold increase ≥ 30 were identified. The XBPs (i.e., PDIA6 and CFL2) responsible for the regulation of protein binding were up-regulated, and those (i.e., TUBB and MX1) responsible for the regulation of catalytic activity were up-regulated in the activated LX-2.

PDIA6 is a protein that belongs to the protein disulfide isomerase (PDI) family and it is involved in the folding of disulphide bonded proteins.³⁴⁻³⁶ The enzymatic formation, breakage, and subsequent rearrangement of cysteine linkages

are crucial to protein structure and function and primarily mediated by members of PDI family.^{32,37,38} Currently, increasing evidence supports an important role for misfolded proteins in the pathogenesis of numerous diseases including diabetes, Alzheimer disease, Parkinson disease, and both alcoholic and non-alcoholic liver disease.^{35,39}

High density lipoprotein (HDL) is a complex and heterogeneous assembly of proteins and lipids. Approximately 75% of the protein content of HDL is APOA1, which serves as the primary protein scaffolding on which the lipid cargo-carrying particle is built.⁴⁰⁻⁴³ Several clinical intervention studies employing either direct infusion of HDL forms or infusion of extracorporeally delipidated HDL or apoA1 have shown anti-atherosclerotic effects.^{44,45} In this study, PDIA6 and APOA1 were selected for further verification in the sera of patients compared with those of normal using western blotting and serum microarrays. Finally, PDIA6 and APOA1 as biomarker candidates were assessed, which show a higher discrimination (AUCs = 0.8985, $p < 0.0001$) relative to APOA1 (AUCs = 0.8738, $p < 0.0001$) in sera of patients.

Conflict of interest

The authors declare that there are no conflicts of interest.

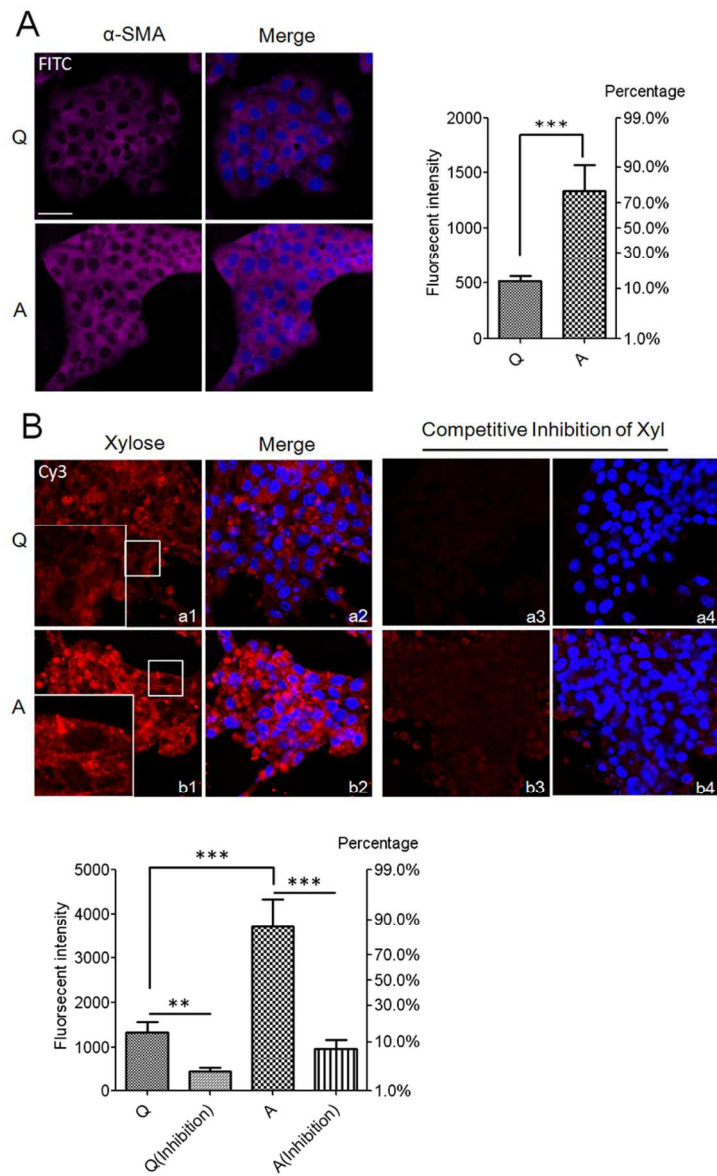
Acknowledgements

We thank Dr. Jihong Cui for collection of images using laser scan confocal microscope. This work is supported by National Natural Science Foundation of China (Grant No. 81372365), Natural Science Basic Research Plan of Shaanxi Province (Grant No.2014JQ3099) and NWU Graduate Innovation and Creativity Funds (Grant No.YZZ14005).

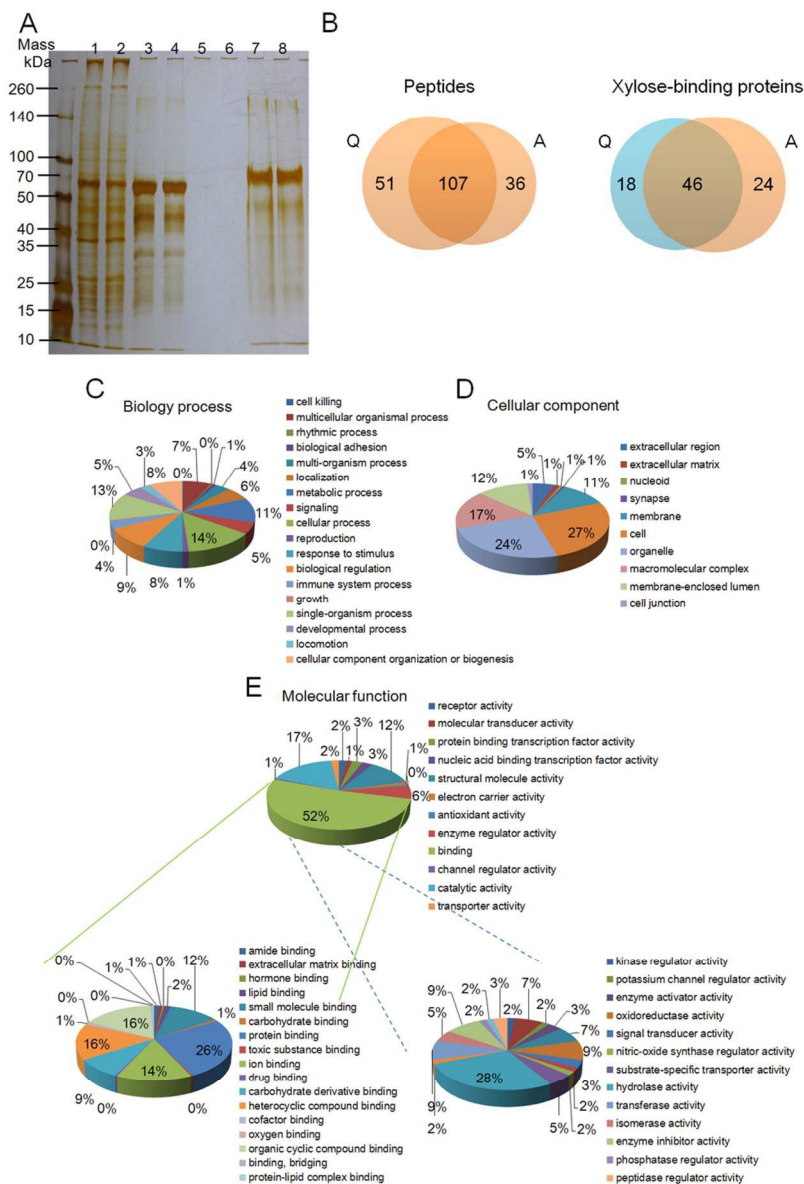
References

1. A. Varki, R.D. Cummings, J.D. Esko, H.H. Freeze, P. Stanley and C.R. Bertozzi, *Essentials of Glycobiology*, 2009, 2nd edition.
2. Y. Zhong, X. Qin, H. Du, L. Dang and Z. Li, *Progress in biochemistry and biophysics*, 2014, **41**, 1173-1181.
3. A. Yan and W.J. Lennarz, *Journal of Biological Chemistry*, 2005, **280**, 3121-3124.
4. T.B. Geijtenbeek and S.I. Gringhuis, *Nature reviews immunology*, 2009, **9**, 465-479.
5. F.T. Liu, *Immunology Today*, 1993, **14**, 486-490.
6. X. Song, Y. Lasanajak, L.J. Olson, M. Boonen, N.M. Dahms, S. Kornfeld, R.D. Cummings and D.F. Smith, *Journal of Biological Chemistry*, 2009, **284**, 35201-35214.
7. P.R. Crocker, J.C. Paulson and A. Varki, *Nature reviews immunology*, 2007, **7**, 255-266.
8. S. Song and C. Park, *Journal of Bacteriology*, 1997, **179**, 7025-7032.
9. H. Weicker and D. Grasslin, *Nature*, 1966, **212**, 715.
10. G. Yang, T. Cui, Y. Wang, S. Sun, T. Ma, T. Wang, Q. Chen and Z. Li, *Proteomics*, 2013, **13**, 1481-1498.
11. R. Khankal, J.W. Chin and P.C. Cirino, *Journal of Biotechnology*, 2008, **134**, 246-252.
12. M. Erbezniak, H.J. Strobel, K.A. Dawson and C.R. Jones, *Journal of Bacteriology*, 1998, **180**, 3570-3577.
13. C. Ahlem, W. Huisman, G. Neslund and A.S. Dahms, *Journal of Biological Chemistry*, 1982, **257**, 2926-2931.
14. D.W. Zhang, Y.X. Zhao, D. Wei, Y.L. Li, Y. Zhang, J. Wu, C. Chen, H. Tang, W. Zhang, L. Gong, Y. Han, Z.N. Chen and H. Bian, *Journal of Hepatology*, 2012, **57**, 1283-1291.
15. R. Bataller and D.A. Brenner, *Journal of clinical investigation*, 2005, **115**, 209-218.
16. D. Schuppan and Y.O. Kim, *Journal of clinical investigation* 2013, **123**, 1887-1901.
17. Y. Qin, Y. Zhong, L. Dang, M. Zhu, H. Yu, W. Chen, J. Cui, H. Bian and Z. Li, *Journal of Proteomics*, 2012, **75**, 4114-4123.
18. Y. Zhong, Y. Qin, L. Dang, L. Jia, Z. Zhang, H. Wu, J. Cui, H. Bian and Z. Li, *Proteomics*, 2015, **15**, 3283-3295.
19. Y. Li, J. Wu, D. Wei, D.W. Zhang, H. Feng, Z.N. Chen and H. Bian, *Liver International*, 2009, **29**, 593-602.
20. Y. Zhong, J. Zhang, H. Yu, J. Zhang, X.X. Sun, W. Chen, H. Bian and Z. Li, *Biochemical and biophysical research communications*, 2015, DOI: 10.1016/j.bbrc.2015.11.055.
21. Y. Qin, Y. Zhong, M. Zhu, L. Dang, H. Yu, Z. Chen, W. Chen, X. Wang, H. Zhang and Z. Li, *Journal of proteome research*, 2013, **12**, 2742-2754.
22. Y. Zhong, H. Yu, Y. Qin, L. Dang, Q. Jian and Z. Li, *Protocol Exchange*, 2015, doi:10.1038/protex.2015.028
23. Y. Zhong, Y. Qin, H. Yu, J. Yu, H. Wu, L. Chen, P. Zhang, X. Wang, Z. Jia, Y. Guo, H. Zhang, J. Shan, Y. Wang, H. Xie, X. Li and Z. Li, *Scientific Reports* 2015; **5**: 8971.
24. A. Conesa and S. Götz, *International Journal of Plant Genomics*, 2008, **2008**, 619832.
25. A. Conesa, S. Götz, J.M. Garcia-Gómez, J. Terol, M. Talón and M. Robles, *Bioinformatics*, 2005, **21**, 3674-3676.
26. J. Ye, L. Fang, H. Zheng, Y. Zhang, J. Chen, Z. Zhang, J. Wang, S. Li, R. Li, L. Bolund and J. Wang, *Nucleic acids research*, 2006, **34**, 293-297.
27. D.W. Huang, B.T. Sherman, Q. Tan, J. Kir, D. Liu, D. Bryant, Y. Guo, R. Stephens, M.W. Baseler, H.C. Lane, R.A. Lempicki, *Nucleic acids research*, 2007, **35**, 169-175.
28. KEGG: Kyoto Encyclopedia of Genes and Genomes. Available at: <http://www.genome.jp/kegg/> (Accessed: 20th November 2014).
29. Motif-x. Available at: <http://motif-x.med.harvard.edu/> (Accessed: 20th November 2014)
30. A. Michalski, E. Damoc, O. Lange, E. Denisov, D. Nolting, M. Müller, R. Viner, J. Schwartz, P. Remes, M. Belford, J.J. Dunyach, J. Cox, S. Horning, M. Mann and A. Makarov, *Molecular & Cellular Proteomics*, 2012, **11**, O111.013698.
31. Subcellular location of PDIA6—The Human Protein Atlas. Available at: <http://www.proteinatlas.org/ENSG00000143870-PDIA6/subcellular> (Accessed: 7th January 2015)
32. J. Groenendyk, Z. Peng, E. Dudek, X. Fan, M.J. Mizianty, E. Dufey, H. Urra, D. Sepulveda, D. Rojas-Rivera, Y. Lim, H. Kim do, K. Baretta, S. Srikanth, Y. Gwack, J. Ahnn, R.J. Kaufman, S.K. Lee, C. Hetz, L. Kurgan, M. Michalak, *Science Signaling*, 2014, **7**, ra54.
33. Subcellular location of APOA1—The Human Protein Atlas. Available at: <http://www.proteinatlas.org/ENSG00000118137-APOA1/subcellular> (Accessed: 7th January 2015).
34. L. Ellgaard and L.W. Ruddock, *EMBO reports*, 2005, **6**, 28-32.
35. J. Galligan and D. Petersen, *Galligan and Petersen Human Genomics*, 2012, **6**, 6.
36. C. Appenzeller-Herzog and L. Ellgaard, *Biochim Biophys Acta* 2008, **1783**, 535-548.
37. C. Turano, S. Coppari, F. Altieri and A. Ferraro, *Journal of cellular physiology*, 2002, **193**, 154-163.
38. X.M. Fu and B.T. Zhu, *Journal of steroid biochemistry and molecular biology*, 2009, **115**, 20-29.

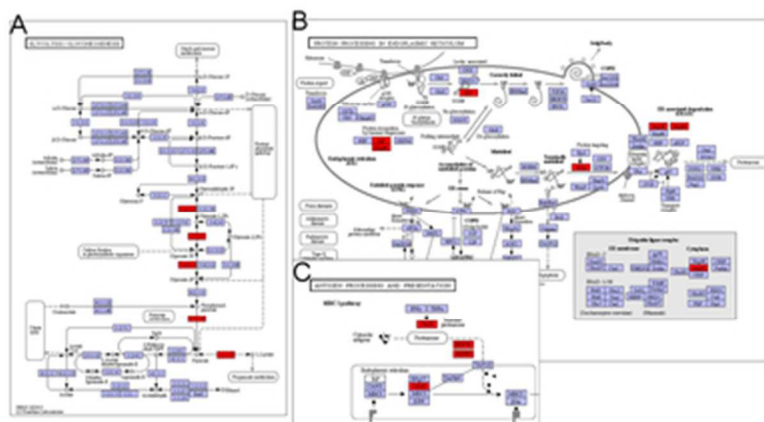
39. J.D. Malhotra and R.J. Kaufman, *Seminars in cell & developmental biology*, 2007, **18**, 716-731.
40. M. Navab, S.T. Reddy, B.J. Van Lenten and A.M. Fogelman, *Nature Reviews Cardiology*, 2011, **8**, 222-232.
41. P.J. Barter, S. Nicholls, K.A. Rye, G.M. Anantharamaiah, M. Navab and A.M. Fogelman, *Circulation research*, 2004, **95**, 764-772.
42. A.V. Khera, M. Cuchel, M. de la Llera-Moya, A. Rodrigues, M.F. Burke, K. Jafri, B.C. French, J.A. Phillips, M.L. Mucksavage, R.L. Wilensky, E.R. Mohler, G.H. Rothblat and D.J. Rader, *The New England Journal of Medicine*, 2011, **364**, 127-135.
43. D. Duffy and D.J. Rader, *Nature Reviews Cardiology*, 2009, **6**, 455-463.
44. T. Gordon, W.P. Castelli, M.C. Hjortland, W.B. Kannel and T.R. Dawber, *American journal of medicine*, 1977, **62**, 707-714.
45. Y. Huang, J.A. DiDonato, B.S. Levison, D. Schmitt, L. Li, Y. Wu, J. Buffa, T. Kim, G.S. Gerstenecker, X. Gu, C.S. Kadiyala, Z. Wang, M.K. Culley, J.E. Hazen, A.J. DiDonato, X. Fu, S.Z. Berisha, D. Peng, T.T. Nguyen, S. Liang, C.C. Chuang, L. Cho, E.F. Plow, P.L. Fox, V. Gogonea, W.H. Tang, J.S. Parks, E.A. Fisher, J.D. Smith and S.L. Hazen, *Nature Medicine*, 2014, **20**, 193-203.



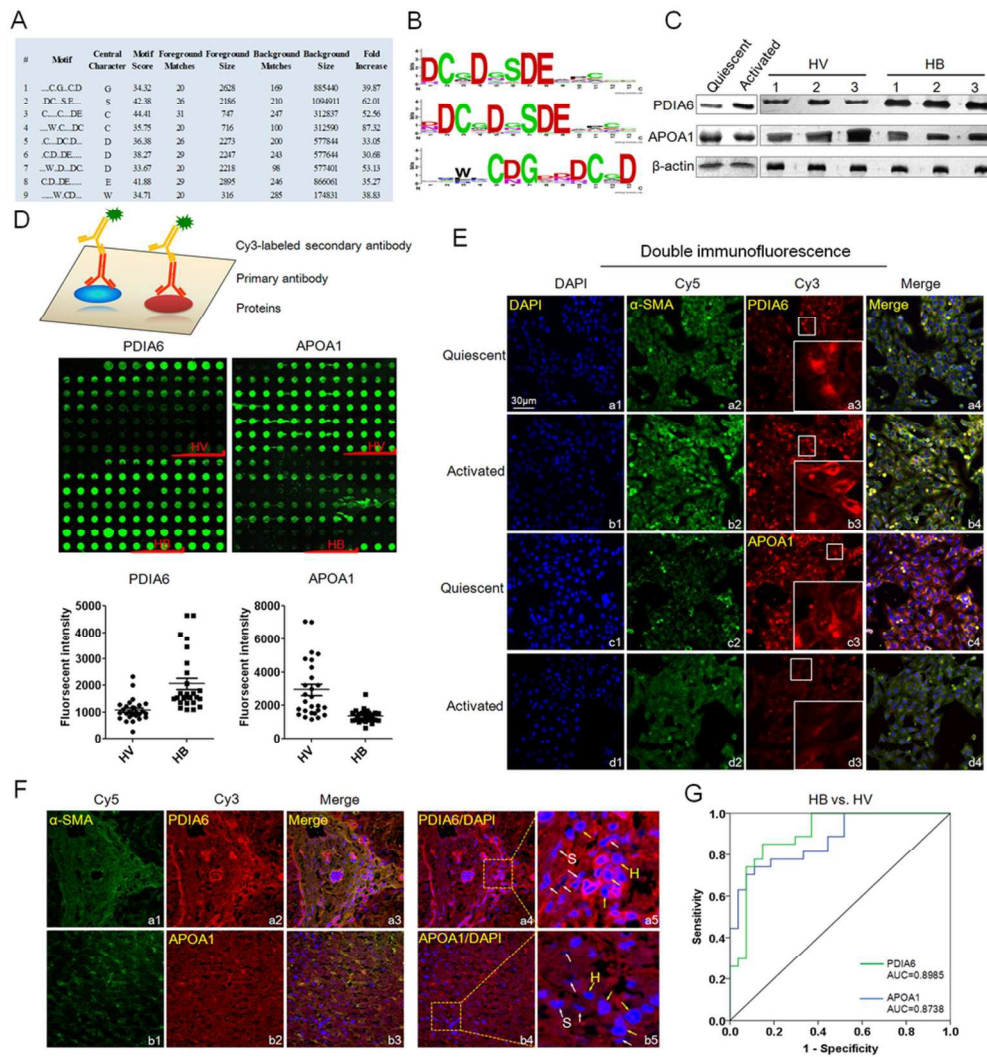
34x55mm (600 x 600 DPI)



44x62mm (600 x 600 DPI)



16x9mm (600 x 600 DPI)



43x46mm (600 x 600 DPI)